2025 IEEE 37TH INTERNATIONAL CONFERENCE ON MICROELECTRONIC TEST STRUCTURES, MARCH 24-27, SAN ANTONIO, TX, USA

Methodology and Test Structures for Studying β-Ga_2O_3 Dielectric and Contact Interfaces

A. A. Gruszecki
Department of Materials Science and Engineering
The University of Texas at Dallas
Richardson, TX, USA
adam.gruszecki@utdallas.edu

J. Roy
Department of Materials Science and Engineering
The University of Texas at Dallas
Richardson, TX, USA
joy.roy@utdallas.edu

K. S. Agrawal
Tyndall National Institute
University College Cork
Cork, Ireland
khushabu.patil@tyndall.ie

P. La Torraca
Tyndall National Institute
University College Cork
Cork, Ireland
paolo.latorraca@tyndall.ie

K. Cherkaoui
Tyndall National Institute
University College Cork
Cork, Ireland
karim.cherkaoui@tyndall.ie

P. K. Hurley
Tyndall National Institute
University College Cork
Cork, Ireland
paul.hurley@tyndall.ie

R. M. Wallace
Department of Materials Science and Engineering
The University of Texas at Dallas
Richardson, TX, USA
rmwallace@utdallas.edu

C. D. Young
Department of Materials Science and Engineering
The University of Texas at Dallas
Richardson, TX, USA
chadwin.young@utdallas.edu

2025 IEEE 37th International Conference on Microelectronic Test Structures (ICMTS) | 979-8-3315-3169-0/25/$31.00 ©2025 IEEE | DOI: 10.1109/ICMTS63811.2025.11068900

***Abstract*— An outline of versatile device structures and test methodologies is provided to streamline the fabrication and characterization of β-Ga_2O_3 and other novel semiconductor materials for the purpose of investigating gate oxide and metal contact interfaces. β-Ga_2O_3/Al_2O_3 metal-oxide-semiconductor capacitors (MOSCAPs) and β-Ga_2O_3/Ti/Au transfer length method (TLM) structures are fabricated for preliminary investigation of dielectric trapping and contact properties as a function of processing. Multifrequency C-V measurements of MOSCAPs show negligible differences in charge trapping at or near the oxide interface following ultraviolet-ozone (UV-O_3) surface pretreatment. Additionally, I-V TLM characterization demonstrates improvements in ohmic contact properties after an O_2 plasma surface cleaning prior to metallization.**

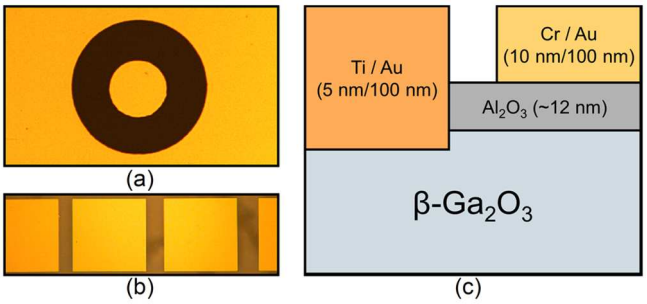

Fig. 1. Optical micrograph depicting the top side of (a) MOSCAP with 50 μm diameter dot size and (b) TLM structures ($L = W = 500$ μm). (c) The full device stack shown as a cross-sectional schematic.

I. Introduction

When investigating new semiconductor technologies, it is important to have access to straightforward and modifiable device processing and test methodologies for preliminary experimental work, as they provide an avenue for ensuing comprehensive studies with a fundamental understanding of various material interfaces. While this work has a particular focus on beta-Gallium Oxide (β-Ga_2O_3) device characterization, the enclosed test methodologies are also intended to be suitable for incipient interface studies of other novel semiconductors. β-Ga_2O_3 is an emerging ultra-wide bandgap semiconductor that shows great promise as a next generation power device technology. Due to its high electric field breakdown [1], considerable Baliga's figure of merit [2], and availability of conventional bulk single crystal growth [3], which exceed the performance and wafer manufacturing limitations of other wide bandgap semiconductors such as SiC or GaN, β-Ga_2O_3 is an attractive choice for future high-power and harsh environment electronic applications.

While considerable research efforts have already been enacted to identify suitable gate dielectrics (Al_2O_3, HfO_2, SiO_2) [4] and ohmic contacts (Ti/Au, Ti/Al/Ni/Au) [5] for β-Ga_2O_3, this work provides an outline for developing further improvements to these interfaces by utilizing simple, common test structures that are easily modifiable within the fabrication flow. Test structures include metal-oxide-semiconductor capacitors (MOSCAPs) and transfer length method (TLM) contacts. With the proper test methodology, device properties such as specific contact resistivity ρ_c, interface trap density D_{it}, and flatband voltage V_{fb} can subsequently be extracted as a function of processing conditions using established I-V and C-V characterization techniques to provide further insight into future process development optimization. In this initial study, several reactive oxygen treatments on various β-Ga_2O_3 interfaces are explored. These processes are known to remove organic contaminants and generate surface states, which may affect gate oxide bonding/interface behavior and ohmic contact charge transport.

This work was supported by the National Science Foundation under Grant ECCS 2154535 at The University of Texas at Dallas and by Research Ireland under Grant 12/US/3755 at Tyndall National Institute through the US-Ireland Research and Development Partnership. *(Corresponding author: Chadwin D. Young.)*

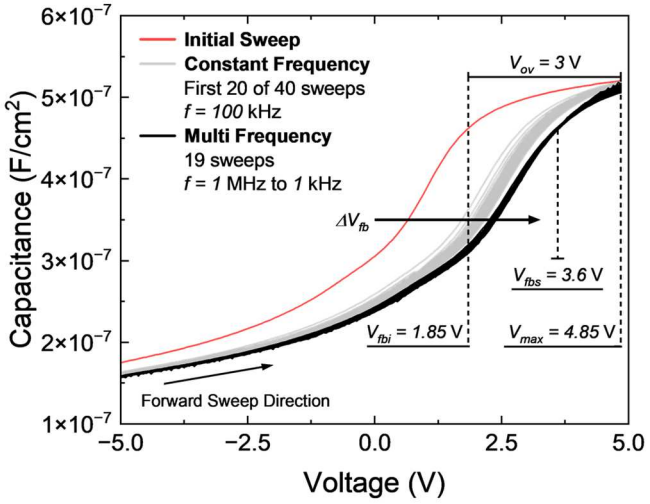

Fig. 2. An example depicting the full C-V test methodology. The initial sweep is used to calculate V_{fbi} and N_d which establishes V_{max}. Constant frequency sweeps are executed to saturate bulk oxide traps, after which multifrequency C-V is performed to determine D_{it} and near-interfacial trapping properties.

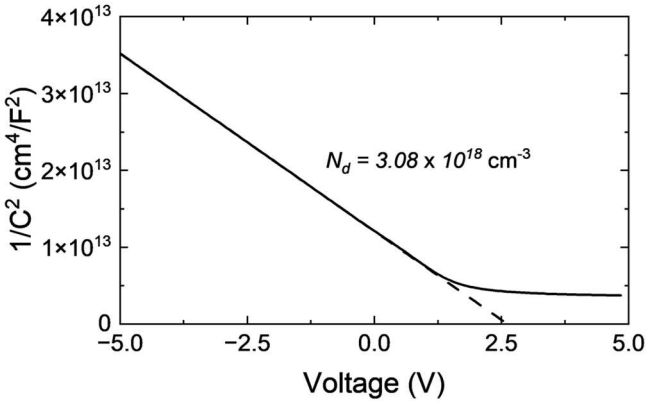

Fig. 3. An example $1/C^2$ vs. V plot used to calculate N_d in bulk β-Ga_2O_3. A least squares linear fit is executed on datapoints in the depletion region of the device's initial C-V sweep.

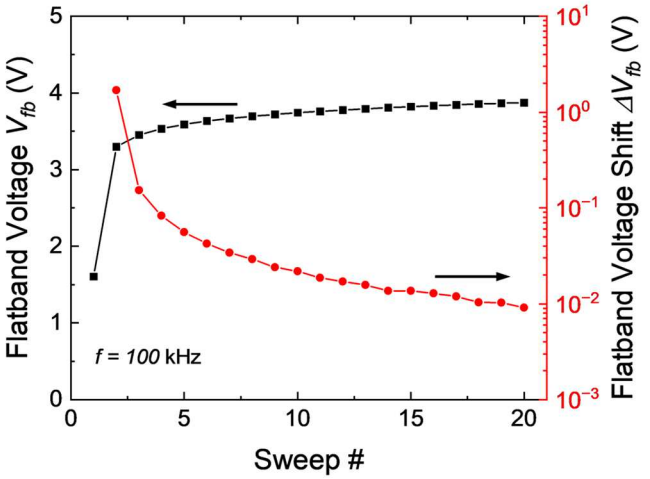

Fig. 4. An example of the cumulative flatband voltage shift observed in β-Ga_2O_3/Al_2O_3 MOSCAPs during successive constant frequency (f = *100* kHz) measurements. Bulk oxide traps within the Al_2O_3 are saturated and the resulting ΔV_{fb} becomes negligible within tens of sweeps.

II. Experimental

Two sample splits were prepared: the first compares MOSCAPs with and without an ultraviolet-ozone (UV-O_3) pretreatment (CAP A and CAP B, respectively), and the second compares TLM structures with and without an O_2 plasma surface treatment prior to metallization (TLM A and TLM B, respectively); with exception of this single process step, all other processing conditions were identical between samples. Bulk β-Ga_2O_3 ($\bar{2}01$) wafers, acquired from Novel Crystal Technology, were diced into 5 x 5 mm^2 pieces. A heavily doped (background doping $N_d \approx 3 \times 10^{18}$ cm^{-3}) substrate was used for device fabrication to facilitate better ohmic contact properties in the absence of selective doping processing. Samples were prepared using a standard organic and piranha clean and 10:1 HF treatment. After the initial cleaning, CAP A received a UV-O_3 pretreatment under oxygen ambient (oxygen pressure $P_{O2} = 1000$ mbar) to remove surface carbon contamination. Next, the sample was transferred to a Picosun R200 plasma-enhanced atomic layer deposition (PEALD) tool and approximately 12 nm of Al_2O_3 was thermally grown using trimethylaluminum (TMA) and H_2O as precursors at 300 °C, where oxide thickness t_{ox} was further verified via ellipsometry. Topside substrate contacts and TLM structures were then defined by conventional photolithography and a BCl_3 inductively coupled plasma (ICP) reactive ion etch (RIE). TLM A received an additional 1-minute 60 W O_2 plasma treatment at 260 mbar prior to metallization. Ohmic contacts were formed by depositing 5 nm /100 nm Ti/Au via e-beam evaporation followed by a 1-minute 470 °C rapid thermal anneal (RTA) in N_2. Subsequent lithography and e-beam evaporation of 10 nm /100 nm Cr/Au were conducted to form the metal gates of MOSCAP structures. Optical micrographs of the fabricated test structures and their cross-sectional schematic are shown in Fig. 1. I-V and C-V characterization was performed using a Keithley 4200 Semiconductor Characterization System (SCS) and B1500A Semiconductor Device Parameter Analyzer on a FormFactor/Cascade Summit manual probe station.

III. Results and Discussion

An advantage of the mesa capacitive test structure is that it shares the top substrate surface with the TLM structures. This ensures that any surface treatments performed during fabrication are identical across all substrate contacts. The Al_2O_3 layer acts as both the gate dielectric for MOSCAPs and a passivation layer for TLM structures during processing, protecting the β-Ga_2O_3 from additional contamination prior to etching. Device measurements are evenly distributed across the sample surface to identify any device-to-device (D2D) variation; this may include nonuniform t_{ox}, N_d, interfacial and oxide trapping distributions, or other features related to device fabrication.

A. MOSCAP Characterization

An important consideration when testing unoptimized MOSCAP devices is ensuring a constant overdrive voltage V_{ov} to maintain a comparable electric field across each individual gate oxide. Oxide defect densities and distributions can vary across a sample, resulting in D2D variation with respect to band bending and the potential drop across the gate dielectric. A constant $V_{ov} = 3$ V is promoted by performing an initial C-V sweep on pristine MOSCAPs from depletion to accumulation up

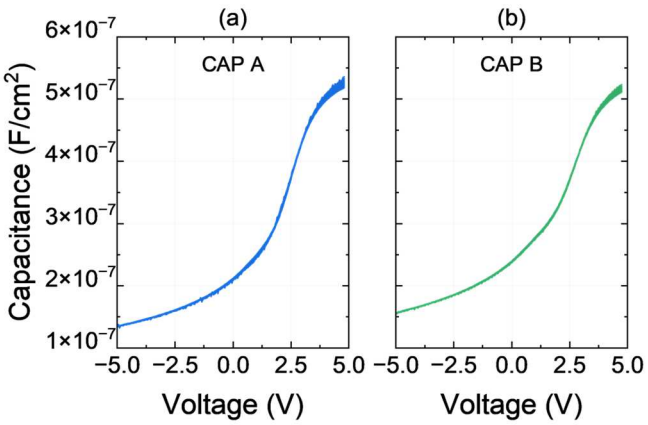

Fig. 5. An example of multifrequency C-V curves for samples with (a) UV-O_3 pretreatment and (b) no surface pretreatment. Capacitance measurements utilize long integration time and span 19 frequencies, ranging from 1 MHz to 1 kHz.

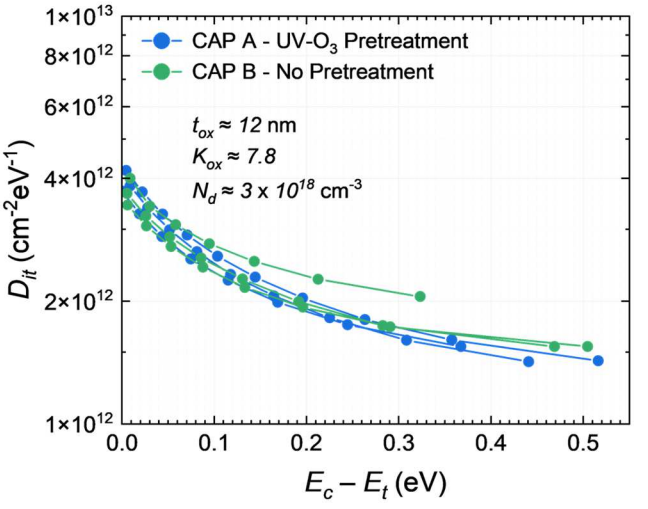

Fig. 6. D_{it} plotted as a function of trap energy relative to the conduction band for 9 sites between both samples. D_{it} is determined via the conductance method. There is minimal change in interface trapping following the UV-O_3 pretreatment.

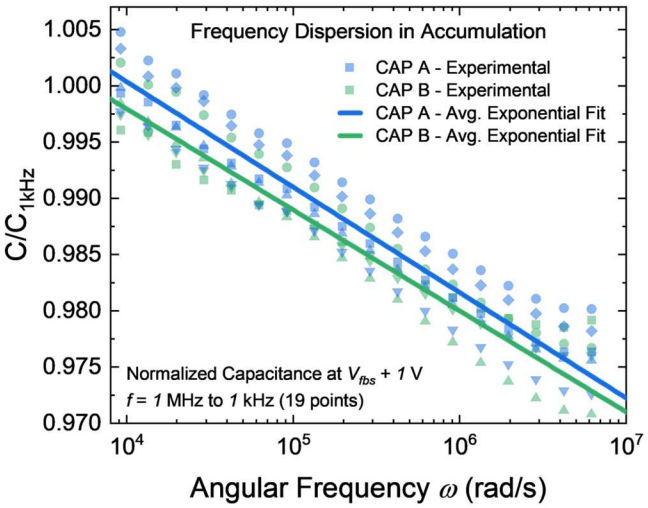

Fig. 7. Normalized accumulation capacitance evaluated at V_{fbs} + *1* V is plotted as a function of frequency for 9 sites between both samples. Exponentially dependent frequency dispersion, represented by the slope of the data fit, is associated with near-interfacial oxide traps.

to a maximum voltage V_{max}. The initial flatband voltage V_{fbi}, shown in Fig. 2, is dynamically calculated from device and material parameters via the function feature of the SCS and used to evaluate $V_{max} = V_{fbi} + V_{ov}$ via the following three equations:

$$N_d = \frac{2}{K_s \varepsilon_0 q A^2 \left(dC^{-2}/dV\right)}, \tag{1}$$

$$\lambda_D = \sqrt{\frac{K_s \varepsilon_0 k_B T}{q^2 N_d}}, \tag{2}$$

and

$$C_{fb} = \frac{C_{ox}(K_s \varepsilon_0 A/\lambda_D)}{C_{ox} + (K_s \varepsilon_0 A/\lambda_D)}, \tag{3}$$

where K_s, ε_0, q, A, λ_D, k_B, T, C_{fb} and C_{ox} are the relative permittivity of the semiconductor (β-Ga_2O_3), vacuum permittivity, elementary charge, gate area, extrinsic Debye length, Boltzmann's constant, temperature, flatband capacitance, and oxide capacitance, respectively. N_d is determined from the reciprocal slope of the $1/C^2$-V curve (Fig. 3) and verifies a uniform doping distribution, which is a critical assumption made when utilizing the depletion approximation. It is noted that the valid region of extraction for substrate doping is not limited by inversion, as the β-Ga_2O_3 is in deep depletion for the negative bias region of the CV response (further addressed later in this section).

Next, a series of constant frequency (CF) C-V measurements is executed at 100 kHz. Al_2O_3, alongside other high-k dielectrics, is well known for having considerable bulk oxide traps that gradually shift V_{fb} and, consequently, the threshold voltage of a device following elapsed stress. A positive voltage shift, identified by ΔV_{fb}, may lead to inaccuracies when extracting oxide trap properties from multifrequency (MF) data. Approximately 40 consecutive voltage sweeps are performed to saturate defect states, leading to a saturated flatband voltage V_{fbs}. The impact of cumulative forward sweeping on V_{fb} in β-Ga_2O_3/Al_2O_3 MOSCAPs is illustrated in Fig. 4. MF C-V is performed immediately after CF measurements to minimize any detrapping; an example comparison of MF C-V between CAP A and CAP B is shown in Fig. 5. D_{it}, which is sensitive to surface treatments and dielectric deposition conditions, typically results in frequency dispersion (FD) within the depletion region of MF C-V. D_{it} was extracted from MF data via the conductance method [6] using the following equations,

$$\frac{G_p}{\omega} = \frac{\omega C_{ox}^2 (G_m - G_t)}{G_m^2 + \omega^2 (C_{ox} - C_m)^2} \tag{4}$$

and

$$D_{it} = \max \frac{2.5}{q}\left(\frac{G_p}{\omega}\right), \tag{5}$$

where G_p, ω, C_m, G_m and G_t are the equivalent parallel conductance, angular frequency, measured capacitance, measured conductance, and tunneling conductance, respectively. D_{it} can be further evaluated as a function of trap energy, shown in Fig. 6, with the energy level of interface states being defined as

$$E_c - E_t = \frac{E_g}{2} + q\varphi_s - q\varphi_b, \tag{6}$$

where $E_c - E_t$, E_g, φ_s, and φ_b are the interface trap energy relative to the conduction band, semiconductor bandgap energy, semiconductor surface potential, and semiconductor bulk potential, respectively. Equation (6) can be solved by first calculating φ_b from material properties, where

$$\varphi_b = k_B T \cdot \ln\left(\frac{N_d}{n_i}\right), \tag{7}$$

and the intrinsic carrier density n_i is defined as

$$n_i = 2\left(\frac{\sqrt{m_e m_h}k_B T}{2\pi\hbar^2}\right)^{3/2} exp\left(-\frac{E_g}{2k_B T}\right), \tag{8}$$

m_e and m_h being the electron and hole effective masses, respectively. By employing the depletion approximation, φ_s can be expressed in terms of gate voltage V_g (normalized by V_{fb}),

$$\varphi_s = V_\delta\left(\sqrt{1 + \frac{V_g - V_{fb}}{V_\delta}} - 1\right)^2 \tag{9}$$

where the potential V_δ is a placeholder variable defined as

$$V_\delta = \frac{qK_s N_d t_{ox}^2}{2K_{ox}^2 \varepsilon_0}, \tag{10}$$

K_{ox} being the relative permittivity of the gate oxide (Al_2O_3). By utilizing (6)–(10), $D_{it}(V)$ as calculated with (4) and (5) can be converted to $D_{it}(E)$; additional details regarding this procedure can be found in [7] and [8].

Exponentially dependent FD in the accumulation region, as depicted in Fig. 7, is generally attributed to slow near-interfacial traps which are less sensitive to high frequencies [9]. Minimal differences between the MF C-V response of CAP A and CAP B, including values of D_{it} and other trap-related properties, are observed. Residual contamination inside the ALD chamber sourced from metal-organic precursors most likely impeded the effectiveness of UV-O_3 treatment in oxidizing or removing surface contamination. As UV-O_3 treatment is known to remove

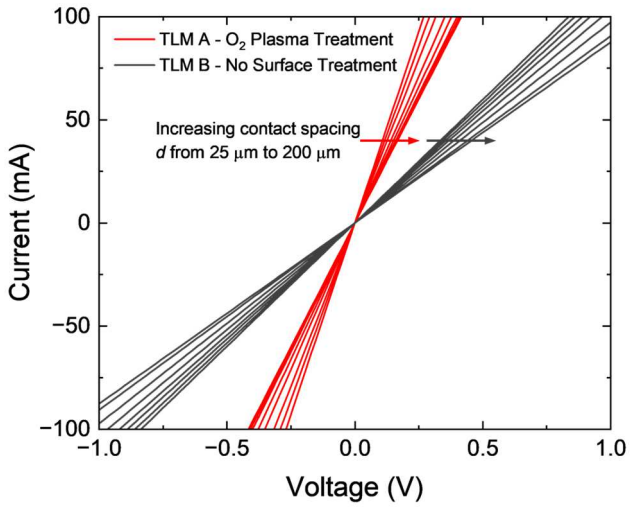

Fig. 8. I-V measurements of TLM structures between each adjacent pair of contacts. Both samples demonstrate ohmic properties, however the additional O_2 plasma surface treatment performed on TLM A improved the total resistance.

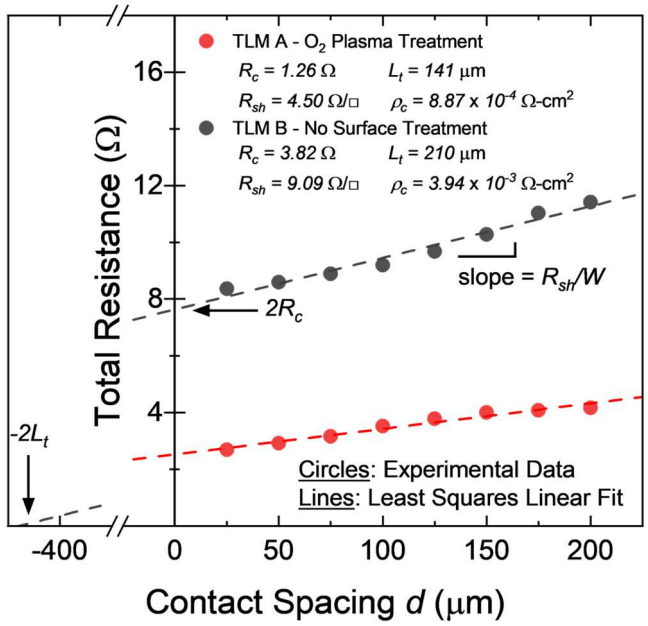

Fig. 9. TLM resistance measurements plotted vs. contact spacing. L_t, R_c, and R_{sh} can be extracted from the x-intercept, y-intercept, and slope of a linear fit, respectively.

adventitious surface carbon, these results may suggest that an additional modification is required to the pretreatment methodology.

B. TLM Characterization

TLM structures are a useful tool for determining various substrate and contact interface properties, including contact resistance R_c, sheet resistance R_{sh}, transfer length L_t, and ρ_c. When selecting a mask for a TLM contact interface study, the appropriate contact size should be taken into consideration. Differences in contact area, among other device dimensions, are known to affect ρ_c calculations and introduce uncertainty [10]. Fig. 8 shows the resistance measurements between each

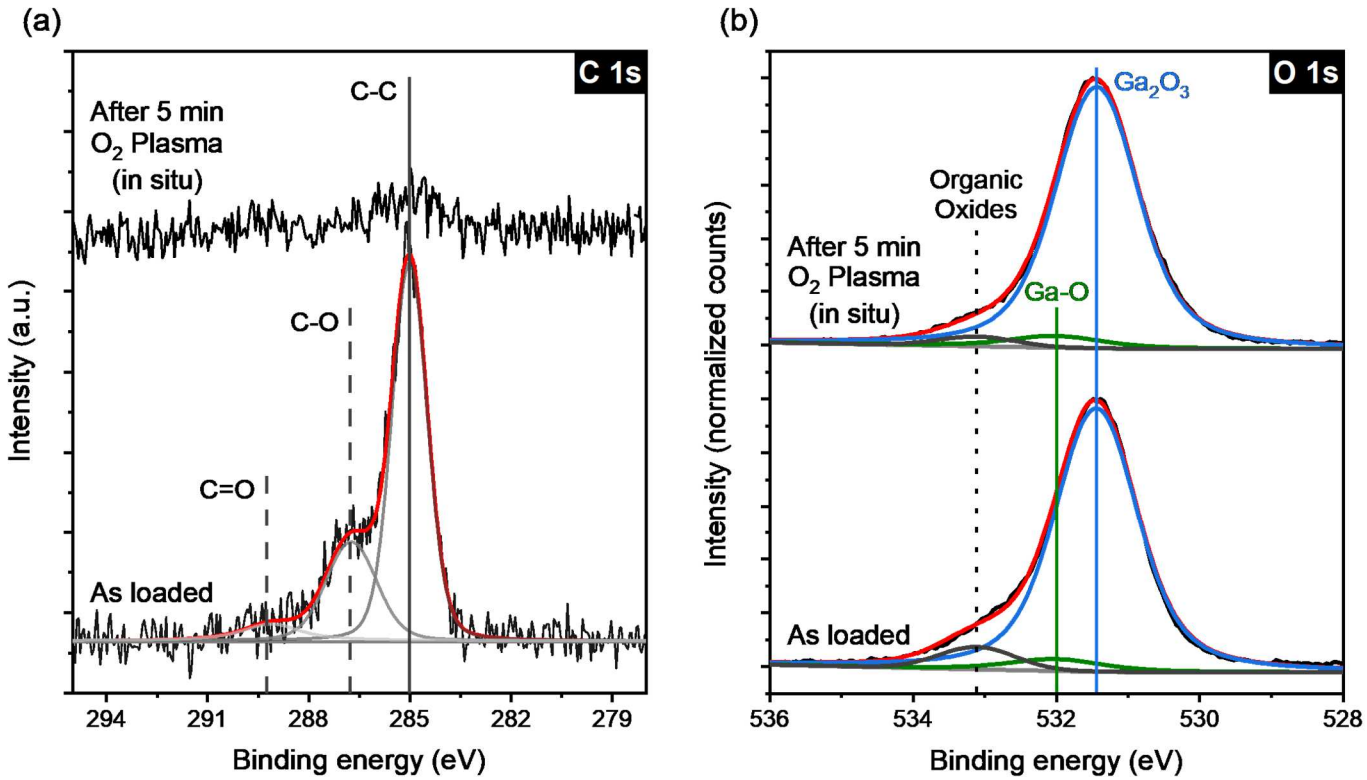

Fig. 10 *In situ* XPS of bulk β-Ga_2O_3 substrate. (a) C 1*s* and (b) O 1*s* before and after 5 minutes of O_2 plasma treatment showing the removal of organic impurities from the surface.

adjacent pair of contacts, where contact dimensions $L = W = 500$ µm for both TLM A and TLM B. By plotting the total measured resistance as a function of contact spacing, various contact properties can be extracted from the linear fit (Fig. 9) and ρ_c is calculated using the following equation:

$$\rho_c = \frac{R_c L_t W}{\coth(L/L_t)}. \tag{11}$$

The full procedure for extracting aforementioned resistive properties is described in [11]. TLM A demonstrates lower R_c, R_{sh}, and ρ_c, which may suggest that performing reactive oxygen surface treatments prior to metallization facilitates better contact formation between Ti and β-Ga_2O_3. As the R_{sh} extraction methodology does not distinguish between resistances underneath and between the contacts, the large discrepancy between both samples may be the result of significant changes in the surface chemistry at the β-Ga_2O_3/Ti interface following surface treatment—especially considering that the regions between TLM contacts are passivated by Al_2O_3.

Fig. 10 demonstrates C 1*s* and O 1*s* core level spectra before and after O_2 plasma treatment on the β-Ga_2O_3 surface prior to oxide deposition. Organic impurities (C-C/C-O) sourced from the *ex situ* transfer process are visible in the initial scan. After 5 minutes of O_2 plasma exposure, signals from C 1*s* went down close to the XPS detection limit—consistent with the reduction of organic oxides in O 1*s*. O_2 plasma treatment has previously been demonstrated to remove carbon contaminants [12] and generate a chemically active oxide layer for improved adhesion [13] (alongside the BCl_3 etch). We speculate that the resulting oxygen-terminated β-Ga_2O_3 surface in the contact regions of TLM A may promote greater bonding between oxygen and Ti, aiding the formation of a conductive Ti-TiO_x region following RTA [14].

Additionally, due to the implementation of a highly doped bulk substrate, L_t is quite large for both samples at around 200 µm. This necessitates large contact pads since a contact length notably lower than L_t will result in Schottky contact behavior. Excessive current spreading also leads to further uncertainty in R_c extractions; however, a self-consistent test methodology is still useful to compare different fabrication processes.

IV. Conclusion

MOSCAPs and TLM structures were fabricated with minimal processing to study the effects of reactive oxygen treatments on the electrical characteristics of multiple β-Ga_2O_3 interfaces. By utilizing the right test methodology, basic device parameters can be easily and rapidly extracted to improve process development for novel semiconductors. In this study, the implementation of UV-O_3 pretreatment prior to ALD demonstrated minimal impact on β-Ga_2O_3/Al_2O_3 interface properties. Organic contaminants are possibly reintroduced to the β-Ga_2O_3 surface from the ALD system which hinders improving the gate oxide interface. TLM structures showed an improvement in contact properties following the O_2 plasma surface treatment, suggesting that this is a valuable step to include in future device processing. However, the impact of reactive oxygen treatments on the β-Ga_2O_3 surface should be

further corroborated with more fundamental studies, including physical characterization and device modeling, in future work.

REFERENCES

[1] G. Jessen *et al.*, "Toward realization of Ga2O3 for power electronics applications," in *2017 75th Annual Device Research Conference (DRC)*, 2017, pp. 1–2. doi: 10.1109/DRC.2017.7999397.

[2] B. J. Baliga, "Semiconductors for high-voltage, vertical channel field-effect transistors," *J Appl Phys*, vol. 53, no. 3, pp. 1759–1764, Mar. 1982, doi: 10.1063/1.331646.

[3] Z. Galazka *et al.*, "On the bulk β-Ga2O3 single crystals grown by the Czochralski method," *J Cryst Growth*, vol. 404, pp. 184–191, 2014, doi: https://doi.org/10.1016/j.jcrysgro.2014.07.021.

[4] P. H. Carey, F. Ren, D. Hays, B. P. Gila, and S. Pearton, "13 - Band alignments of dielectrics on (−201) β-Ga2O3," in *Gallium Oxide*, S. Pearton, F. Ren, and M. Mastro, Eds., Elsevier, 2019, pp. 287–311. doi: https://doi.org/10.1016/B978-0-12-814521-0.00013-0.

[5] Y.-W. Huan *et al.*, "Recent Advances in β-Ga2O3–Metal Contacts," *Nanoscale Res Lett*, vol. 13, no. 1, p. 246, 2018, doi: 10.1186/s11671-018-2667-2.

[6] E. H. Nicollian and J. R. Brews, *MOS (metal oxide semiconductor) physics and technology*. New York: Wiley, 1982.

[7] S. M. Sze and K. K. Ng, "Metal-Insulator-Semiconductor Capacitors," in *Physics of Semiconductor Devices*, 2006, pp. 197–240. doi: https://doi.org/10.1002/9780470068328.ch4.

[8] W. R. Frensley, "The Metal-Oxide-Semiconductor Structure," in *Understanding Electron Devices*. Unpublished.

[9] D. M. Fleetwood, "'Border traps' in MOS devices," *IEEE Trans Nucl Sci*, vol. 39, no. 2, pp. 269–271, 1992, doi: 10.1109/23.277495.

[10] S. Grover, S. Sahu, P. Zhang, K. O. Davis, and S. K. Kurinec, "Standardization of Specific Contact Resistivity Measurements using Transmission Line Model (TLM)," in *2020 IEEE 33rd International Conference on Microelectronic Test Structures (ICMTS)*, 2020, pp. 1–6. doi: 10.1109/ICMTS48187.2020.9107911.

[11] D. K. Schroder, "Contact Resistance and Schottky Barriers," in *Semiconductor Material and Device Characterization*, 2005, pp. 127–184. doi: https://doi.org/10.1002/0471749095.ch3.

[12] F. González-Posada *et al.*, "Surface cleaning and preparation in AlGaN/GaN-based HEMT processing as assessed by X-ray photoelectron spectroscopy," *Appl Surf Sci*, vol. 253, no. 14, pp. 6185–6190, 2007, doi: https://doi.org/10.1016/j.apsusc.2007.01.016.

[13] X. Ma, W. Mu, T. Hou, Y. Dong, Y. Li, and Z. Jia, "Low-cost O2 plasma activation assisted direct bonding of β-Ga2O3 and Si substrates in air," *Mater Sci Semicond Process*, vol. 179, p. 108512, 2024, doi: https://doi.org/10.1016/j.mssp.2024.108512.

[14] J. Bae, H.-Y. Kim, and J. Kim, "Contacting Mechanically Exfoliated β-Ga2O3 Nanobelts for (Opto)electronic Device Applications," *ECS Journal of Solid State Science and Technology*, vol. 6, no. 2, p. Q3045, 2017, doi: 10.1149/2.0091702jss.